Continuous two-dimensional releases from an elevated source

Paul F. Linden and John E. Simpson
Department of Applied Mathematics and Theoretical Physics, University of Cambridge, Silver Street, Cambridge CB3 9EW, UK

This work examined the continuous escape of a dense fluid through an elevated line slit and its impact with the ground. The effects of the initial momentum of the release on both the descending flow and the spreading dense cloud were also investigated. Dimensional analysis was used to relate the velocity, depth and dilution of the spreading gravity current to the source conditions, and the theory was confirmed by a series of experiments with salt solution in a water tank. Observations of the concentration fields obtained by digitizing flow visualisation are presented.

(Keywords: release; plume; dense gas)

In this paper the continuous escape of dense fluid from a two-dimensional elevated source, into uniform stationary surroundings, is considered. Attention is restricted to the case of vertical releases, since releases at angles to the vertical have recently been analysed[1].

The processes to be considered can be divided into three separate regimes: descent (region A), during which the flow behaves as a forced plume; the region (B) of impingement, which may include a hydraulic jump; and a horizontal gravity current stage (C). These stages are illustrated schematically in *Figure 1*. Only the case where the gravity current flow is in an inertia-buoyancy balance is investigated. The two later stages of the gravity current, which include control of the flow by viscous forces[2] and mixing of the fluid by ambient turbulence[3], are not considered.

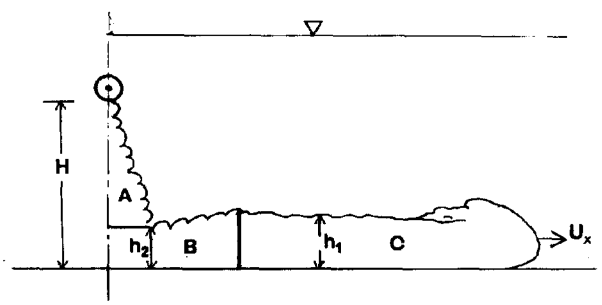

Figure 1 A, descending jet or plume; B, impingement region and hydraulic jump; C, gravity current

Received 12 September 1989
Presented at the First Int. Conf. on Loss of Containment, 12–14 September 1989, London, UK
0950–4230/90/010082–06$3.00

The motion produced by a steady source of buoyancy and momentum is called a forced plume[4]. Near the source, the flow behaves like a jet, but as the excess momentum decreases the flow becomes that of a plume, controlled entirely by buoyancy forces. When the initial front is included the flow is called a starting plume. Extensive laboratory studies on two-dimensional starting plumes were carried out[5], but they did not consider the part played by the momentum flux in the early stages. This aspect was examined in the descent for two-dimensional forced plumes[6], but was restricted to the flow behind the leading front.

The problem of impingement on a plane surface and the subsequent spread in three dimensions of plumes and jets has been studied[7], and dimensional arguments have been given for both finite and continuous three-dimensional discharges. However, the effects of the initial momentum flux were not considered.

Dimensional analysis

Effect of initial excess momentum on descent

It is possible to deduce many of the properties of turbulent buoyant jets from simple dimensional analysis, combined with empirical data from the experiments. In a two-dimensional flow, the dimensions of mass flux, Q, momentum flux, M, and buoyancy flux, B, are

Mass flux $(Q) = L^2T^{-1}$

Momentum flux $(M) = L^3T^{-2}$

Buoyancy flux $(B) = L^3T^{-3}$

where L refers to length, and T refers to time. In a two-dimensional plume in which the source momentum flux is negligible, the simple, dimensionally correct, relationship is

$$z = C_p B^{1/3} t \qquad (1)$$

where B is the buoyancy flux, which is conserved throughout the flow, and z refers to either the descent of the front that leaves the source ($z = 0$) at time $t = 0$, or the distance reached by any material element in the following plume. Therefore, for a plume, the velocity of advance of the front is constant.

In a flow which is dominated by momentum (a jet), dimensional analysis gives

$$z = C_j M^{1/3} t^{2/3} \qquad (2)$$

where C_j is a constant.

The length over which the flow 'forgets' its initial momentum and behaves like a plume, is usually referred to[8] as the 'jet length', L_m, where

$$L_m = C_L M/B^{2/3} \qquad (3)$$

The empirical constants C_p, C_j and C_L are determined experimentally. For a forced plume, in which neither the buoyancy flux nor the mass flux can be neglected, Equations (1) and (2) can be generalized in the form

$$z = C(z/L_m)\, B^{1/3} t \qquad (4)$$

Comparing Equation (4) with Equations (1) and (2), and using Equation (3), the following limiting values are obtained for $C(z/L_m)$

$$\text{plume } (z/L_m \gg 1) \qquad C \rightarrow C_p$$
$$\text{jet } (z/L_m \ll 1) \qquad C \rightarrow C_j^{3/2}\, C_L^{-1/2}\, (L_m/z)^{1/2} \qquad (5)$$

The width b of the flow is proportional to z

$$b = \alpha z \qquad (6)$$

where α is the entrainment constant (≈ 0.1 for both jets and plumes). The plume dilutes as it descends, and the buoyancy (measured by reduced gravity, $g' = g\Delta\rho/\rho$, where $\rho + \Delta\rho$ is the density of the plume and ρ the density of the surroundings) decreases with distance from the source. Dimensional analysis gives

$$g' = C_g(z/L_m) B^{2/3} z^{-1} \qquad (7)$$

Horizontal flow

Dimensional analysis may also be applied to this phase of the flow, and the forms obtained are similar to those for the vertical descent. They are written here in terms of x, the horizontal distance of the front from the point of impact of the plume centre line with the ground, and the time t measured from the time of impact of the initial front.

$$x = C_1(H/L_m)B^{1/3}t$$
$$h_1 = C_2(H/L_m)H$$
$$g' = C_3(H/L_m)B^{2/3}H^{-1} \qquad (8)$$

For horizontal flow, the constants, C_1, C_2 and C_3 depend on the height, H, of the source compared with the jet length, L_m.

Experimental

The perspex tank used was 4.0 m long by 1.0 m wide, and could be filled to a depth of 0.5 m. A schematic view of the apparatus used to introduce the fluid is shown in *Figure 2*. Dense fluid was released from a cylindrical source extending across the width of the tank. The cylinder had a slit pointing downwards and contained a ring of sponge around packed glass balls, to distribute the flow evenly. An outer collar could be rotated round the cylinder, to cover the slit when required. The reservoir above the cylinder enabled air to be bled from the cylinder before a run. The flow was pumped from a reservoir and the flow rate was monitored by means of a gapmeter.

Flow visualization was by shadowgraph and using dye to mark the dense fluid. The flow was recorded using video and still photography. Measurements of dye intensity, averaged across the width of the tank, were obtained by digitizing video images. The digitizer consisted of a grey-scale frame grabber with store. False colour records were displayed on an IBM PC screen and finally copied onto colour-print camera film. During each run, measurements were made of the salinity (and hence the density) of the fluid in the gravity current regime at a single point, using a conductivity probe. This probe was controlled by a microcomputer, sampling at 10 Hz.

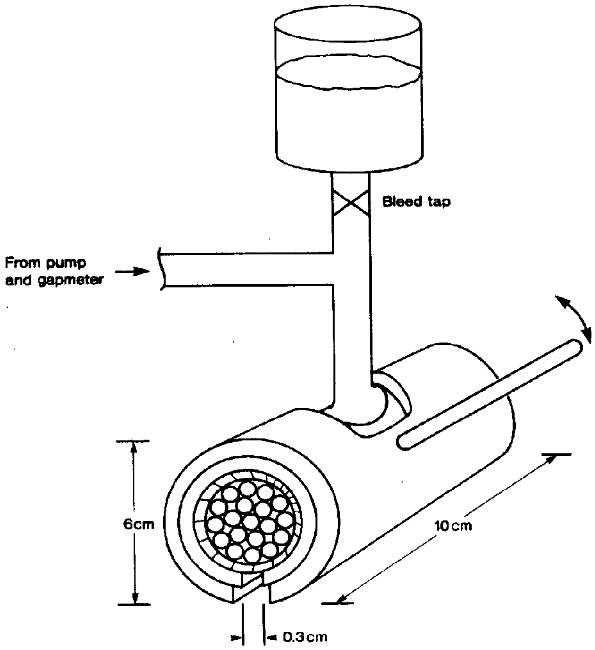

Figure 2 Schematic view of apparatus used to release a steady buoyancy current. The external collar enables the slit to be closed

Qualitative description of the flow

The general features of the flow are shown in *Figure 3*. The front in this starting plume resembles a thermal, and it is followed by a narrower tail that increases in width as it descends. The tail usually shows sideways oscillations, signs of which can be seen in the photographs. In some of the experiments the initial jet regime was short-lived and the flow rapidly attained the nature of a plume. In others, the initial conditions were chosen so the jet regime extended down as far as the ground.

Upon impact with the bottom of the tank, the flow was diverted horizontally. The horizontal flow has many features in common with a classical gravity current: namely a raised head, with Kelvin–Helmholz billows at the front. In some circumstances, additional features such as a hydraulic jump immediately after the region of impingement are seen. Near the point of impact, the horizontal flow exhibits a comparatively rapid increase in height from the initial height, h_0. Beyond this a steady height, h_1, is maintained (see *Figure 1*), except near the elevated turbulent head of the gravity current.

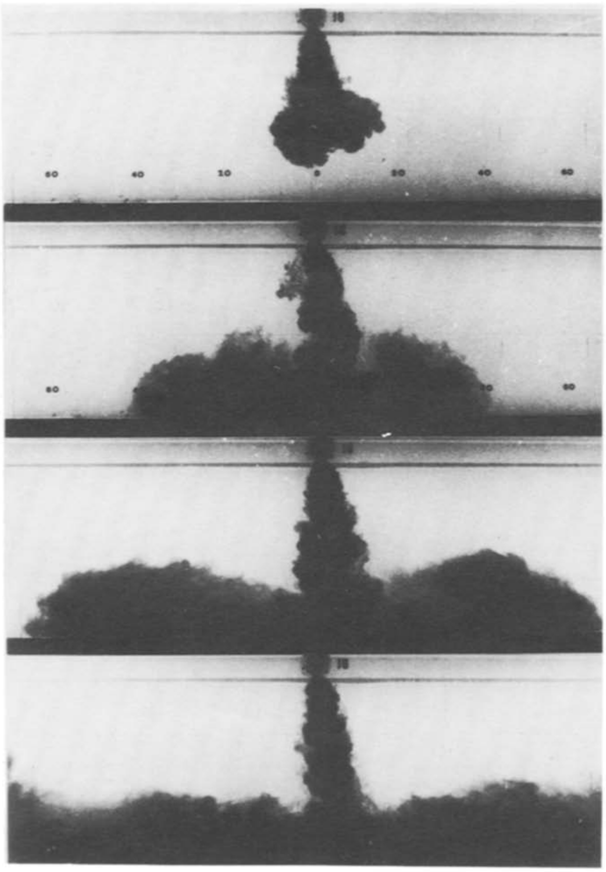

Figure 3 Four views of the descent of the negatively buoyant fluid being released from the container seen at the top. The scale on the photographs is in cm

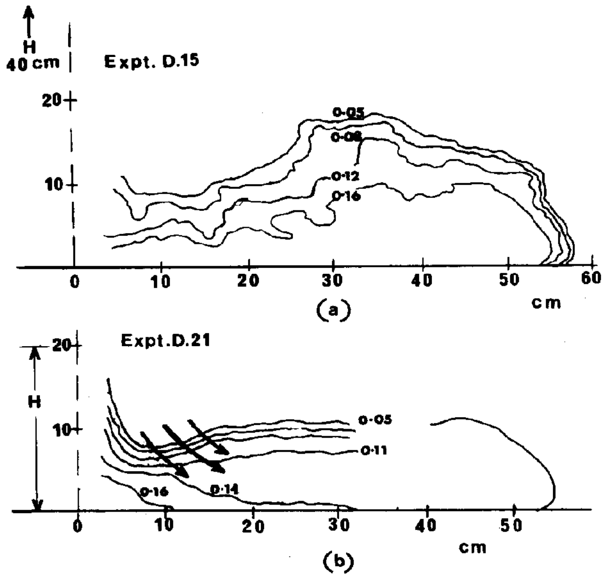

Figure 4 Tracings of constant density surfaces obtained by digitizing video images: a, short jet length $H/L_m = 0.38$: b, large jet length $H/L_m = 4$. The numbers on the contours are values of $100\Delta\rho/\rho$

Figures 4a and *4b* show tracings of the surfaces of constant density for two flows in which the jet length, L_m, is less than and greater than the height H of the source, respectively. In *Figure 4a*, when $L_m/H < 1$, the horizontal flow has features of a classical gravity current with a raised head. However, when $L_m/H > 1$, the raised head is absent and the divergence of density surfaces (indicated by arrows) implies the presence of an entraining region immediately downstream of the impact region. This is probably caused by a hydraulic jump, since the flow is ultimately controlled by the front of the current[2].

Quantitative results

Descent phase

An example of the descent of the front is plotted against time in *Figure 5*. This log-log plot shows that the descent phase has two distinct characteristics: near the source, $z \propto t^{2/3}$, while for larger distances, $z \propto t$. This is as expected for the jet and plume regimes, respectively (see Equations (1) and (2)). The transition occurs at $z = 15$ cm, which suggests that C_L is 1.4 (see Equation (3)). In practice, the transition from jet to plume will be a gradual process, and this is borne out by the compilation of a number of experiments, shown in *Figure 6*. In *Figure 6*, $1/C$ (where $C = C(z/L_m)$ is the dimensionless function in Equation (4)) is plotted against $z/MB^{-2/3}$. The limits for the plume ($z/L_m \gg 1$) and the jet ($z/L_m \ll 1$) – see Equation (5) – are shown as straight lines. The data conform to these expected values very well and from these data we estimate $C_p = 1.2$, $C_j = 1.3$ and $C_L = 1.4$.

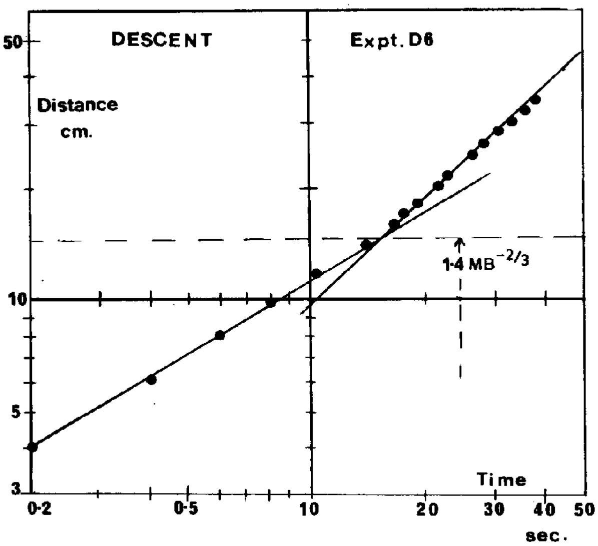

Figure 5 Distance travelled by descending front with time. The log/log plot shows the different velocities in the jet and plume regions. The gradients are 2/3 and 1 respectively

Horizontal spread

Velocity of the final flow. The velocities of the advancing fronts were measured from the video records, and a typical example is shown in *Figure 7*, which shows that the front travels at a constant speed, in accordance with Equation (8). The results for a range of $H/MB^{-2/3}$ from 0.5 to 15 are shown in *Figure 8*, in which values of C_1 determined from data such as those shown in *Figure 7* are plotted. For values of height/jet length ratio > 5, i.e. short jet length, little variation with jet length could be detected and the mean value of C_1 in Equation (8) was 1.08. However, when the jet length became an appreciable part of the total descent, for values of $H/MB^{-2/3}$ between 5 and 1, the value of C was measurably reduced. When the jet regime reached the ground, $H/MB^{-2/3} < 1$, the value of C_1 was ≈ 0.83. The three regimes are marked in *Figure 8* as 'jet', 'transition' and 'plume'.

Height of final flow. The dimensionless relationship expected here is a simple one, $h_1 = C_2(H/L_m)H$, (see Equation (8)). *Figure 9* shows the results from 24 experiments, in which the value of $C_2 = h_1/H$ is plotted against $H/MB^{-2/3}$, the ratio of height to jet length. Although only five points are plotted, each

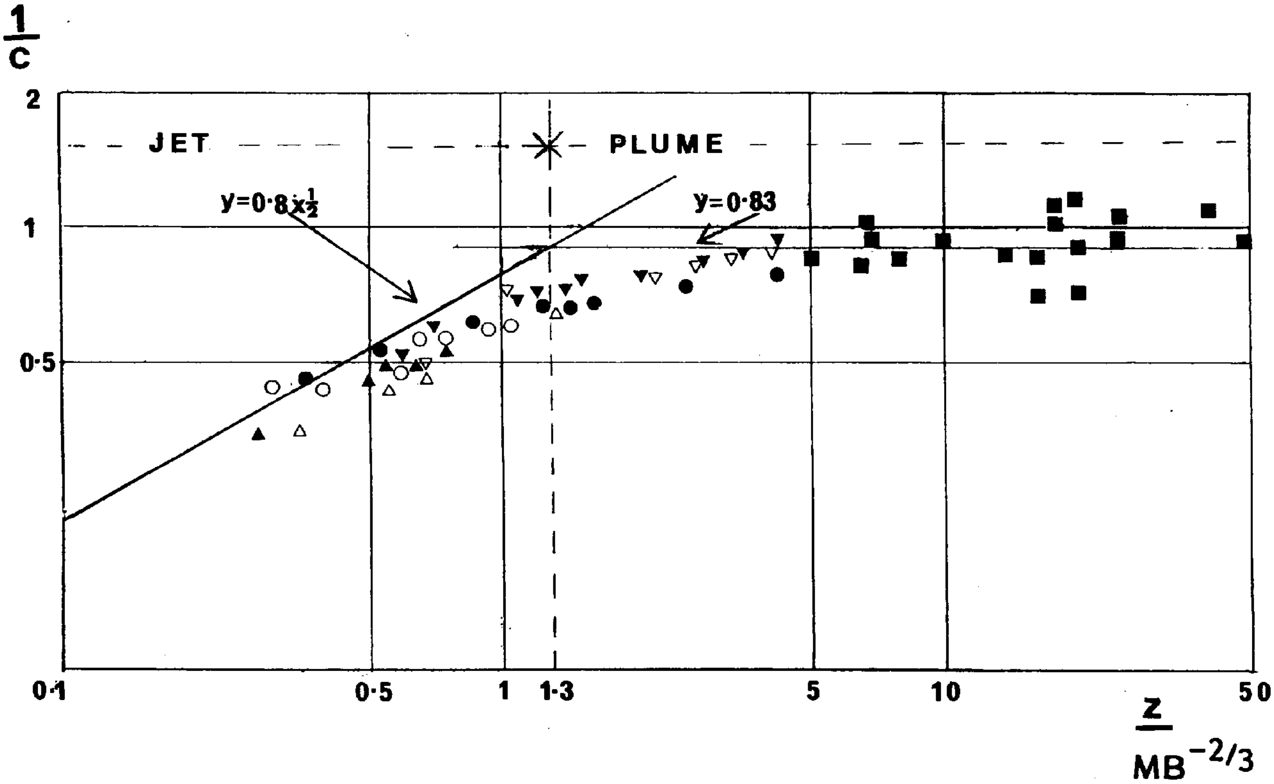

Figure 6 Graph of $1/C$ against $z/MB^{-2/3}$, where $C = C(z/L_m)$ is defined by Equation (4). The straight lines show the expected behaviour in the jet and plume regions

represents the results from several different experiments, but with the same nominal starting conditions. The results show that $C_2 \approx 0.25$, but with a small variation associated with the value of the jet length.

Dilution of final fluid Dimensional analysis (Equation (8)) shows that the final value of g' must be of the form $g' = C_3 B^{1/3} H^{-1}$. To determine the approximate value of C_3, $g'H/B^{1/3}$ is plotted against $H/MB^{-2/3}$ (Figure 10). From digitized images such as those shown in *Figure 4*, it can be seen that there is insignificant mixing downstream of the hydraulic jump, so this final result is well defined. The details of the 24 experiments are shown in *Table 1*. *Table 2* gives the values for C_1, C_2 and C_3 corresponding to the jet, transition, and plume regimes.

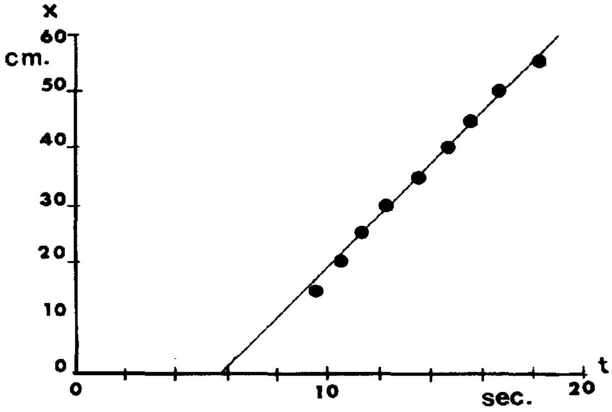

Figure 7 Distance travelled by the front of the horizontal current with time, when $H/MB^{2/3} = 7.4$

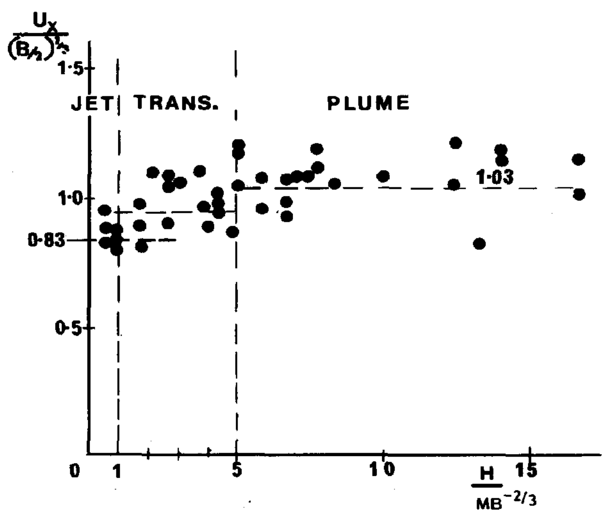

Figure 8 Values of C_1, defined by Equation (8), for the gravity current front in the jet, transition and plume regions

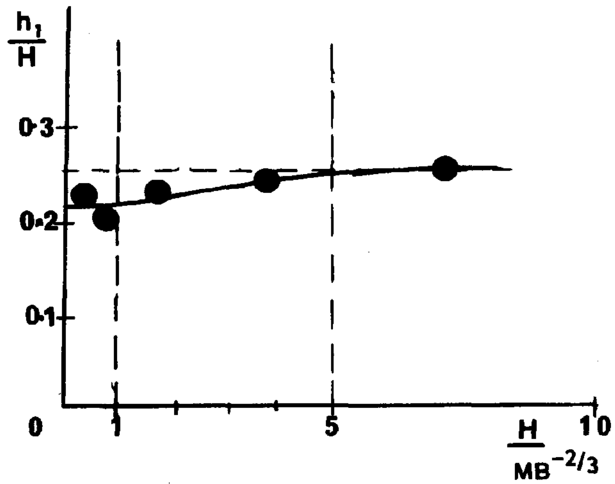

Figure 9 Dimensionless height, $C_2 = h_1/H$, of the final flow

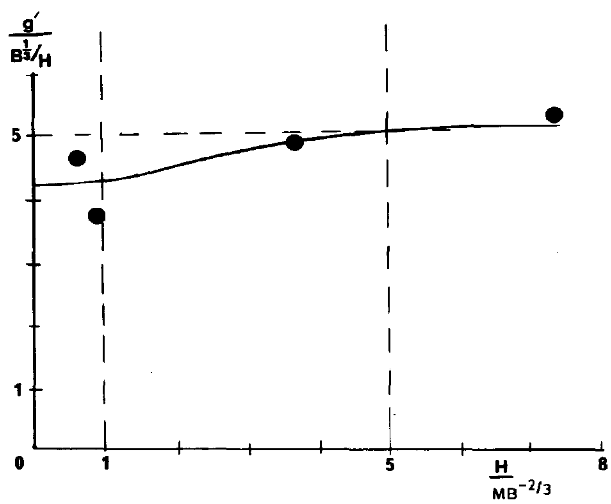

Figure 10 Variation of dilution C_3 (non-dimensional) with jet length. Each point plotted represents the mean of four experimental runs

Conclusions

In this paper we have examined the vertical descent and impact with the ground of negatively buoyant fluid released through a line source. The effects of initial vertical momentum on both the descent of the flow and on its subsequent horizontal spread after impact with the ground are studied. The velocity, depth and dilution of the flow are consistent with a simple dimensional analysis. The form of the appropriate dimensionless functions, and their dependence on the momentum of the source, have been determined. For practical purposes, it is clear that almost all of the dilution occurs during the descent phase and that this is increased significantly as the source momentum increases.

Table 1 Experimental details

Experimental means	B	g'_1	h_1	U	h/H	Fr[a]	$g'_1H/B^{2/3}$	H/L_m	H
a (8)	115	2.68	10.5	5.3	0.24	1.01	4.93	3.7	43
b (4)	69.5	2.0	10.5	4.44	0.25	0.91	5.08	7.4	43
c (4)	48.7	2.45	4	3.02	0.20	0.96	3.75	0.95	20
d (4)	28.2	1.77	4.5	2.70	0.225	0.96	4.72	0.69	20
e (4)	14.2	1.0	4.6	2.12	0.25	0.99	3.32	1.7	20
mean	–	–	–	–	–	0.97	–	–	–

[a] Froude number = velocity/(density × height)$^{1/2}$

Table 2 Values of C_1, C_2 and C_3 corresponding to jet, transition and plume regions

		Jet H/L_m =0.5	Plume H/L_m =5.0	Trans-ition	Approx
Speed, $U = C_1 B^{1/3}$	C_1	0.83	1.05	0.94	1.0
Height, $h_1 = C_2H$	C_2	0.21	0.25	0.23	0.25
Dilution, $g'_1 = C_3 (B^{2/3})/H$	C_3	4.2	5.0	4.6	4.5
$Fr = C_1/(C_2C_3)^{1/2}$	Fr	0.94	0.94	0.94	1

Acknowledgements

The authors thank S. Dalziel for his assistance in the work on the digital display. This work was carried out with the support of the Health and Safety Executive.

References

1 Lane-Serff, G. F., Linden, P. F. and Hillel, M. *J. Fluid Mech.* submitted for publication
2 Simpson, J. E. and Huppert, H. E. *J. Haz. Mat.* submitted for publication
3 Linden, P. F. and Simpson, J. E. *J. Fluid Mech.* 1986, **172**, 481
4 Morton, B. R. *J. Fluid Mech.* 1969, **5**, 151
5 Tsang, G. *Atmos. Environ.* 1970, **4**, 519
6 Kotsovinos, N. E. and List, E. J. *J. Fluid Mech.* 1977, **81**, 25
7 Turner, J. S. in 'Buoyancy effects in fluids', Cambridge University Press, Cambridge, UK, 1973